J Membrane Biol (2007) 219:49–61
DOI 10.1007/s00232-007-9060-x

HERG1 Currents in Native K562 Leukemic Cells

María S. Cavarra · Silvana M. del Mónaco · Yanina A. Assef · Cristina Ibarra · Basilio A. Kotsias

Received: 18 June 2007 / Accepted: 18 June 2007 / Published online: 1 September 2007

Abstract The human ether-a-go-go related gene (HERG1) K^+ channel is expressed in neoplastic cells, in which it was proposed to play a role in proliferation, differentiation and/or apoptosis. K562 cells (a chronic myeloid leukemic human cell line) express both the full-length (herg1a) and the N-terminally truncated (herg1b) isoforms of the gene, and this was confirmed with Western blots and coimmunoprecipitation experiments. Whole-cell currents were studied with a tail protocol. Seventy-eight percent of cells showed a HERG1-like current: repolarization to voltages negative to -40 m*V* produced a transient peak inward tail current, characteristic of HERG1 channels. Cells were exposed to a HERG-specific channel blocker, E4031. Half-maximal inhibitory concentration (IC_{50}) of the blocker was 4.69 nM. The kinetics of the HERG1 current in K562 cells resembled the rapid component of the native cardiac delayed rectifier current, known to be conducted by heterotetrameric HERG1 channels. Fast and slow deactivation time constants at -120 m*V* were 27.5 and 239.5 ms, respectively. Our results in K562 cells suggest the assembling of heterotetrameric channels, with some parameters being dominated by one of the isoforms and other parameters being intermediate. Hydrogen peroxide was shown to increase HERG1a K^+ current in heterologous expression systems, which constitutes an apoptotic signal. However, we found that K562 HERG1 whole-cell currents were not activated by H_2O_2.

Keywords HERG1 K^+ channel · H_2O_2 · E4031 · K562

M. S. Cavarra · S. M. del Mónaco · Y. A. Assef · B. A. Kotsias (✉)
Laboratorio de Neurofisiología, Instituto de Investigaciones Médicas Alfredo Lanari, Universidad de Buenos Aires-CONICET, C. de Malvinas 3150, Buenos Aires 1427, Argentina
e-mail: kotsias@mail.retina.ar

C. Ibarra
Laboratorio de Fisiopatogenia, Facultad de Medicina, Universidad de Buenos Aires, Paraguay 2155, Buenos Aires 1121, Argentina

Introduction

The ether-a-go-go-related gene 1 (erg1) codes the conducting α-subunit of the voltage-activated K^+ channel ERG1 (Warmke & Ganetzky, 1994). Four α-subunits co-assemble to form the conducting core of ERG channels; each α-subunit consists of six transmembrane α-helical domains and intracellular N and C termini (Warmke & Ganetzky, 1994). The human erg1 gene (herg1), located on chromosome 7, is composed of 15 exons (Curran et al., 1995; Itoh et al., 1998) and encodes for at least four isoforms: HERG1a, HERG1b, HERG-USO and HERG-sm. HERG1a was the first characterized isoform and is the longest one since the others have shorter N-terminal (1b) or C-terminal (USO, sm) regions (Warmke & Ganetzky, 1994; Kupershmidt et al., 1998; Lees-Miller et al., 1997; Shoeb, Malykhina & Akbarali, 2003).

HERG1 was found to be abundantly expressed in the heart, where it is responsible for the rapid component of the delayed rectifier K^+ current (I_{Kr}), playing a critical role in normal cardiac repolarization (Sanguinetti et al., 1995; Curran et al., 1995; Li et al., 1996). Moreover, it has been linked to the long QT syndrome type 2 (LQT2), an inherited or acquired cardiac disorder (Curran et al., 1995; Sanguinetti et al., 1995).

Several kinetic and pharmacological features define both expressed HERG1 and native I_{Kr} currents. First, HERG1

channels slowly open when depolarized to positive voltages but inactivate extremely quickly, thus suppressing the efflux of intracellular K^+ during the depolarization. Second, upon repolarization, channels rapidly recover from inactivation, producing a resurgent current as they revisit the open state before slowly closing. Net ion movement through these channels over a depolarization-hyperpolarization cycle is inward when isomolar K^+ concentrations are used at both sides of the membrane. Third, they are selectively blocked by methanesulfonanilides like E4031 (Sanguinetti & Jurkiewicz, 1990; Sanguinetti et al., 1995; Schönherr & Heinemann, 1996; Spector et al., 1996a, 1996b; Wang et al., 1997a).

Several functions have been attributed to native ERG1 channels in excitable cells, such as regulation of cardiac and smooth muscle action potential, spike frequency adaptation in neurons, oxygen sensing and modulation of hormone release in neuroendocrine cells (*for review, see* Schwarz & Bauer, 2004). It has also been observed that its pattern of expression varies during normal development of cardiac and nervous tissues, suggesting a role in differentiation-maturation (Wang et al., 1996; Crociani et al., 2000).

Expression of erg1 was also found in cancerous cells, derived from both excitable and nonexcitable tissues. In these cells, modulation of proliferation, apoptosis, differentiation and migration by this channel has been also postulated (*for review, see* Wang, 2004; Arcangeli, 2005). In particular, overexpression of the herg1 gene has been reported in various types of neoplastic hematopoietic cells (Smith et al., 2002; Pillozzi et al., 2002), although electrophysiological characterization of kinetic parameters of HERG1-like currents was not reported. For this reason, functional studies of HERG1 currents could be of particular interest, contributing to a better knowledge of the role they play in cellular signaling in tumor cells.

The human myeloid cell line K562, established by culturing leukemic cells from the pleural effusion of a patient in blastic transformation, is composed mainly of undifferentiated blasts (Lozzio & Lozzio, 1975; Klein et al., 1976), which can be induced to differentiate along the erythroid lineage in response to various stimuli (Hoffman et al., 1979; Rutherford, Clegg & Weatherall, 1979; Tsiftsoglou et al., 1991). These cells are also able to acquire resistance to several cytotoxic drugs (Hamada & Tsuruo, 1988). Thus, the K562 cell line can serve as a useful model for channel studies at different stages of maturation or multidrug resistance (Assef & Kotsias, 2002; Assef et al., 2003, 2005).

In the present work, we study the expression of HERG1 channels and characterize the kinetics and drug sensitivity of HERG1 native currents in undifferentiated K562 cells. We find that K562 cells express both the full-length (herg1a) and the N-terminally truncated (herg1b) isoforms of the gene, which coassemble to form fully active heterotetrameric channels with distinctive properties.

Materials and Methods

Cell Culture

The K562 cell line (American Type Culture Collection, Rockville, MD) was grown in RPMI 1640 culture medium (HyClone, Logan, UT), supplemented with 10% fetal bovine serum (FBS; GIBCO, Carlsbad, CA). Cells were kept at 37°C in humid air (5% CO_2).

The HEK293 cell line stably transfected with the herg1a cDNA (HEK-HERG cells), kindly provided by Dr. C. January (University of Wisconsin, Madison, WI), was used as positive control of herg1 expression in reverse-transcriptase polymerase chain reaction (RT-PCR) experiments. HEK-HERG cells were maintained and propagated in Dulbecco's modified Eagle medium (DMEM, Hyclone) supplemented with 10% FBS and G418 400 μg/ml (A. g. Scientific, Inc., San Diego, CA) at 37°C in humid air (5% CO_2).

PCR

Total RNA from wild-type K562 or HEK-HERG cells was isolated using the SV Total RNA isolation system. DNase was used during the total RNA extraction. Reverse transcription of mRNA was achieved by incubation of total RNA with oligo(dT) primers, Moloney murine leukemia virus reverse transcriptase (MMLV-RT) and dNTPs in the presence of RNAsin at 42°C for 60 min. All reagents and enzymes were purchased from Promega (Madison, WI).

Expression of total herg1 or herg1a and herg1b isoforms in K562 cells was evaluated using the primers detailed in Table 1, which amplify specific sequences of these transcripts from the whole population of retrotranscribed cDNA. PCR consisted of 30–50 cycles of 94°C for 1 min, 58°C for 1 min, 72°C for 1 min and 6 min at 72°C for final extension. Some of these primers amplify sequences comprised of more than one exon and thus served as genomic DNA contamination controls. ß-Actin primers (Biodynamics) were used as internal control. RT-PCR products were separated on ethidium bromide-stained 1–3% agar gels in TBE 1x buffer. Images of gels were acquired with Foto Analyst Investigator (Fotodyne, New Berlin, WI). pUC19 DNA/MspI(HpaII) molecular weight marker was a kind gift from Dr. M. Costas (Instituto de Investigaciones Médicas, Alfredo Lanari, Universidad de Buenos Aires, Buenos Aires, Argentina).

Table 1 Data of primer pairs used for PCR experiments

Primer		Product size (bp)	Exon	Recognizes	Reference
Herg1 F	Sequence 5′CTCAAGGCCGTGTGGGACT3′	552	6–7	herg1 S1 domain (both isoforms)	Bauer et al., 2003
Herg1 R	5′CAGGTTGTGCAGCCAGCCGA3′				
Herg1b F	5′CGATTCCAGCCGGGAAGGC3′	361	1b-6	herg1b N terminus	Crociani et al., 2003
Herg1b R	5′TGATGTCCACGATGAGGTCC3′				
herg1a F	5′CTCAACTCCACCTCGGACTC3′	160	5	herg1a N terminus	(PubMed NCBI) NM_000238
herg1a R	5′TGTGGGTTCGCTCCTTTATC3′				
β-actin F	5′CGGAACCGCTCATTGCC3′	289	-		
β-actin R	5′ACCCACACTGTGCCCATCTA3′				

Western Blot

K562 cells were washed with cold phosphate-buffered saline (PBS) and resuspended in a small volume of lysis buffer (50 mM 4-[2-hydroxyethyl]-1-piperazineethanesulfonic acid [HEPES], 250 mM NaCl, 1 mM ethylenediaminetetraacetic acid [EDTA], 1% NP-40 [pH 8], supplemented with a mix of protease inhibitors). Cell lysates were centrifuged at 10,000 rpm for 5 min at 4°C. Total protein in each sample was quantified using the Bradford assay.

For Western blot studies, 100 µg of total proteins from K562 cells were dissolved in loading buffer (4% sodium dodecyl sulfate, 0.125 M Tris-HCl [pH 6.8], 0.2 M dithiothreitol, 0.02% bromophenol blue, 20% glycerol). The preparation was heated to 100°C for 10 min, resolved on 8% polyacrylamide gel and electrotransferred onto Immun-Blot® polyvinylidene difluoride (PVDF) membranes (Bio-Rad, Richmond, CA). These membranes were blocked in Tris-buffered saline (TBS) containing 10% (w/v) nonfat dry milk and 0.05% Tween-20 for 1 h at room temperature and incubated overnight with HERG antibodies. In human tissues two herg transcripts encode proteins differing in their amino-terminal sequences, HERG1a and HERG1b (Jones et al., 2004). We used two isoform-specific antibodies directed to this divergent amino-terminal region which allow us to differentiate the two isoforms. We detected HERG1a using a rabbit polyclonal antibody directed against amino acid residues 140–153 of HERG1a transcript, at a dilution 1:100. For HERG1b, we used a rabbit polyclonal antibody directed against amino acid residues 9–23 of HERG1b transcript, at a dilution 1:1,000. Both antibodies were a kind gift from Dr. Gail Robertson (University of Wisconsin, Madison, WI), who previously demonstrated antibody specificity (Jones et al., 2004). Membranes were then washed with TBS-Tween 0.05% (T-TBS) and incubated with a horseradish peroxidase-conjugated secondary antibody (Vector Laboratories, Burlingame, CA; 1:5,000) for 1 h at room temperature. The bands were detected using an enhanced chemiluminescence system. Each Western blot was carried out at least three times.

Coimmunoprecipitation

After washing K562 with cold PBS, cells were resuspended in 1 ml of lysis buffer (*see above*, "Western Blot"). Cell lysates were incubated for 20 min in ice and centrifuged at 8,000 rpm for 5 min at 4°C. Proteins were immunoprecipitated overnight with HERG1a (1:20) or HERG1b (1:100) antibodies on a rotating platform at 4°C. G-coupled Sepharose beads (10 µl; Pharmacia Biotech, Gaithersburg, MD) were added, and samples were incubated at 4°C for an additional 90 min. Proteins bound to the beads were washed three times with lysis buffer, eluted by boiling the samples in loading buffer, analyzed by sodium dodecyl sulfate-polyacrylamide gel electrophoresis and transferred to PVDF membranes. The membranes were incubated overnight with T-TBS containing 5% bovine serum albumin and the appropriate primary antibody at the concentration reported above. Membranes were then processed as described for Western blot analysis. Controls consisted of a sample with total protein lysate and a sample where total rabbit serum was added to cell lysate instead of primary antibody.

Drugs and Reagents

The membrane-permeable ERG-selective blocker E4031, 1-(2-[6-methyl-2-pyridyl]-ethyl)-4-(4-methylsulfonylaminobenzoyl)piperidine, a methanesulfonanilide (class III antiarrhythmic agent) (Sanguinetti & Jurkiewicz, 1990; Spector et al., 1996b), was purchased from Alomone Labs (Jerusalem, Israel). E4031 was diluted in sterile distilled

water, and a stock solution was kept at −20°C. Bath solution containing E4031 at the desired final concentration was prepared weekly and stored at −4°C. ATP-Mg was purchased from Sigma-Aldrich (St. Louis, MO) and H_2O_2 from Parafarm (Droguería Saporiti, Buenos Aires, Argentia).

Electrical Recordings

The electrical activity of K562 cells was recorded in the whole-cell configuration with standard patch-clamp technology using a PC-501A amplifier (Warner, Hamden, CT). All experiments were performed at room temperature (20–24°C). Stimulation and digitalization of the signal were achieved using Pclamp6.0 software (Axon Instruments, Burlingame, CA). Electrical signals were acquired at 10 kHz and filtered at 1 kHz. Microelectrodes were pulled from standard borosilicate glass (1.5 mm optical density) and fire-polished to a final resistance of 2–4 MΩ when filled with intracellular solution. Gigaseal's resistances (1–10 GΩ) were obtained in standard NaCl bath solution. After whole-cell configuration was attained, the bath solution was replaced by high-K^+ bath solution for current measurements. Currents were measured several times in this solution before any treatment was performed, to assess their stability.

Junction potentials were minor to 5 m*V*; thus, they were not corrected. For measurement of the kinetic parameters of the HERG1-like currents, we carefully corrected pipette and cell capacitance and the series resistance was compensated before each voltage-clamp protocol ramp. Pipette solution contained (mM) K-glutamate 84, KCl 46, $MgCl_2$ 1, Mg-ATP 5, HEPES 10, sucrose 60 and 1,2-bis(*o*-aminophenoxy)ethane-*N,N,N′,N′*-tetraacetic acid (BAPTA) 0.3 (final [Ca^{2+}] 100 nM) (pH 7.4). Standard NaCl bath solution contained (mM) NaCl 150, KCl 5, $CaCl_2$ 1, $MgCl_2$ 1 and HEPES 10 (pH 7.4). High-K^+ bath solution contained (mM) K-glutamate 88, KCl 42, $CaCl_2$ 1, $MgCl_2$ 1, sucrose 34 and HEPES 10 (pH 7.4). Two well-known voltage-clamp protocols commonly used for the study of HERG1 currents were tested in K562 cells. Protocol 1 consisted of a 2-s depolarizing step to +40 m*V* (in order to activate/inactivate HERG1 channels), followed by a family of hyperpolarizing test pulses (from −120 to +40 m*V*), during which inward resurgent tail current was measured. Protocol 2 consisted of a 2-s hyperpolarizing step to −70 m*V* (in order to close HERG1 channels), followed by a family of test pulses from −70 to +40 m*V*, at which voltage-dependent activation/inactivation of the channels occurs, and a final hyperpolarizing step to −120 m*V*, at which tail current values correlate with the proportion of channels that opened in the preceding test pulse.

Data Analysis

The onset of peak tail current (protocol 1) was fitted to a double or single exponential function (for voltages more negative or more positive than −80 m*V*) to determine the time course of recovery from inactivation (Sanguinetti et al., 1995). The fast time constant (τf) accounts for the rapid current increase, caused by recovery from channel inactivation, while the slow time constant (τs) represents the slower current increase due to an overlap of recovery from inactivation with channel deactivation; for this reason, τs is not shown (Sanguinetti et al., 1995). The deactivation time constants were obtained by fitting peak tail current (protocol 1) with a double exponential function from the peak of the resurgent tail current to the steady-state (SS). Voltage dependence of activation (protocol 2) was calculated by fitting normalized peak tail current at −120 m*V* ($I/I_{max} = p_o$) plotted against the preceding test pulse, with a Boltzmann equation of the form $p_o = 1/(1 + e^{(-zF(V_m - V_{0.5})/RT)})$, where p_o represents the open probability, V_m the test voltage, $V_{0.5}$ the membrane potential at which $p_o = 0.5$, F the Faraday constant, R the universal gas constant, T the absolute temperature and z the equivalent gating charge. The fraction of I_{Kr}-like peak current blocked by E4031 (FB) was calculated at −120 m*V* for each drug concentration and fitted with a Hill equation of the form $FB = FB_{max}/[(IC_{50}/Drug)^h + 1]$, where Drug is the E4031 concentration tested, FB_{max} is maximal fractional block, IC_{50} is the E4031 concentration required for half-maximal block and h is the Hill coefficient. Data were expressed as mean ± standard error (SE, n being the number of cells analyzed). For statistical comparison, analysis of variance (ANOVA) or Student's *t*-test was performed. Differences were considered significant at $p < 0.05$.

Results

Expression of herg1 Isoforms in K562 Cells

Total RNA was extracted from K562 and HEK-HERG cells, and RT-PCR experiments were performed using primers specific for the herg1 gene (Bauer et al., 2003). An expected band was detected in both wild-type (WT) K562 and HEK-HERG1 cells (Fig. 1a, b left). The same results were obtained in three independent experiments. The N terminus of ERG1a protein contains a PAS (*Per, Arnt, Sim)* domain, which has been shown to dynamically influence ERG1a gating (Schönherr & Heinemann, 1996; Morais Cabral et al., 1998; Wang et al., 1998). An erg isoform that exhibits a much shorter and unique N-terminal sequence (erg1b) was cloned from mouse and human heart in 1997 (Lees-Miller et al., 1997). Mice or rat ERG1b homotetramers are known to display differential kinetics compared to ERG1a

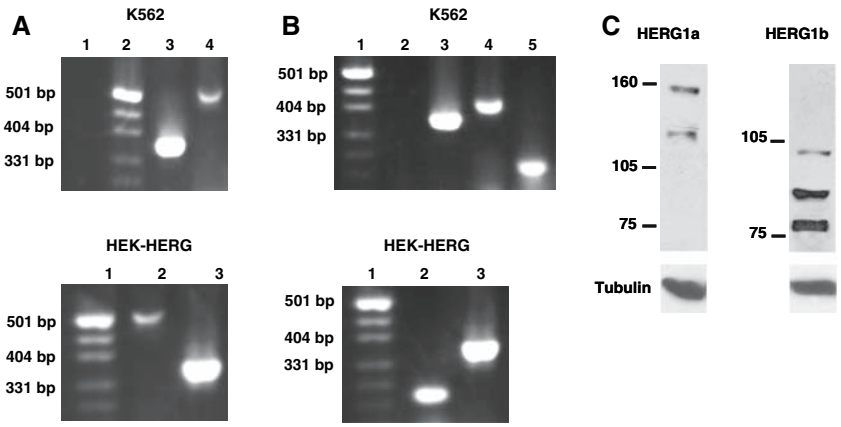

Fig. 1 Expression of HERG1 in K562 cells. **a** RT-PCR products of K562 and HEK-HERG cells obtained with primers "herg1" (detailed in Table 1) were loaded in a 3% agar gel. *Left panel* shows K562 amplification products: *lane 1*, negative control; *lane 2*, molecular weight marker (MW); *lane 3*, ß-actin; *lane 4*, herg1. *Right panel* shows HEK-HERG amplification products: *lane 1*, molecular weight marker; *lane 2*, herg1; *lane 3*, ß-actin. **b** RT-PCR products of K562 and HEK-HERG cells obtained with primers "herg1a" and "herg1b" (detailed in Table 1) were loaded in a 3% agar gel. *Left panel* shows K562 amplification products: *lane 1*, molecular weight marker; *lane 2*, negative control; *lane 3*, ß-actin; *lane 4*, herg1b; *lane 5*, herg1a. *Right panel* shows HEK-HERG amplification products: *lane 1*, molecular weight marker; *lane 2*, herg1a; *lane 3*, ß-actin. **c** Representative Western blot of total protein extracts from K562 cells. *Left blot* shows HERG1a glycoform bands at ~155 and ~135 kDa. *Right blot* shows HERG1b glycosylation states, showing ~95, ~85 and ~80 kDa bands. Tubulin was used as an internal control (57 kDa)

homotetramers or ERG1a/1b heterotetramers (Lees-Miller et al., 1997; London et al., 1997; Kirchberger et al., 2006). Coexpression of HERG1a and HERG1b isoforms has been reported in other leukemic cells (Crociani et al., 2003). We tested if K562 cells express HERG1b by using a previously reported set of primers that recognize its unique N-terminal sequence (Crociani et al., 2003). The expected ≈ 361-bp band was detected in K562 cells (Fig. 1a, right). We also designed primers to amplify a unique N-terminal sequence of the HERG1a isoform and used HERG1a transfected HEK cells (HEK-HERG) to test them. They successfully recognized the expected ≈ 160-bp band in both HEK-HERG and K562 cells (Fig. 1a, b, right).

HERG channels undergo *N*-linked glycosylation, which influences surface membrane expression and functional properties (Zhou et al., 1998; Petrecca et al., 1999; Jones et al., 2004). Using HERG1a and HERG1b isoform-specific antibodies (see "Materials and Methods"), we detected HERG1 channel in K562 cells (Fig. 1c). Western blot analysis showed two bands, of ~155 and ~135 kDa, for HERG1a, which is consistent with the mature and immature HERG1a glycoforms, respectively (Zhou et al., 1998; Petrecca et al., 1999). HERG1b-specific antibody recognized the three expected bands of ~95, ~85 and ~80 kDa, also representing different glycosylated forms (Jones et al., 2004).

HERG1 Currents in WT K562 Cells

Because of the particular kinetics, HERG1 currents are most easily studied as a resurgent "tail" current during steps to very negative potentials after stimulation with a depolarized voltage in order to open the channels. The electrical activity of K562 cells was first recorded with the standard patch-clamp technique in the whole-cell configuration with protocol 1 (see "Materials and Methods") (Fig. 2a). Due to the small current densities of the K562 nonexcitable cells (Assef & Kotsias, 2002; Assef et al., 2003, 2005), a high external potassium concentration was used to increase the K^+ driving force and, thus, the amplitude of the inward HERG1 current at negative potentials (Nernst potential ≈ 0 m*V*) (Spector et al., 1996a; Schönherr & Heinemann, 1996; Smith et al., 2002). Cells were held at a holding potential of 0 m*V*, at which little or no basal current was observed.

In 23 of 104 cells studied, we could not detect I_{Kr}-like currents (Fig. 2b). The rest of the cells (78%) showed an I_{Kr}-like current in high-K^+ bath solution since repolarization to voltages more negative than −40 m*V* produced transient peak inward tail current (Fig. 2c). Amplitude of I_{Kr}-like currents varied greatly between cells, probably due to channel density differences between them. However, this variability was not reduced when normalizing current values to cell capacitance (*data not shown*). To confirm the identity of these I_{Kr}-like currents, K562 cells were exposed to the HERG channel blocker E4031. Drug equilibration across the cell membrane was allowed for at least 3 min since E4031 is known to permeate and act from the intracellular side (Zou et al., 1997). This time is more than sufficient to achieve steady-state block at the 0 m*V* holding potential used by us (Spector et al., 1996b). I_{Kr}-like currents were inhibited by E4031 in 27 out of 29 cells tested.

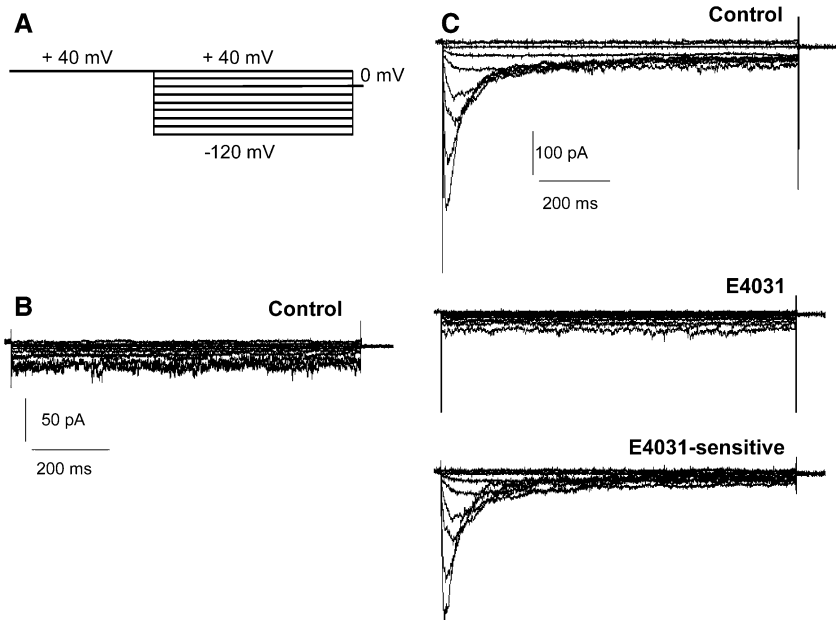

Fig. 2 Functional detection of HERG1 in K562 cells. **a** Graphic representation of protocol 1, which consisted of a 2-s depolarizing step to +40 m*V*, followed by a family of test pulses from −120 to +40 m*V* in 20-m*V* steps. Holding potential was 0 m*V*. **b** Representative current traces obtained with protocol 1 from a K562 cell that does not present I_{Kr}-like currents. Prepulse to +40 m*V* is not shown. **c** Representative current traces obtained with protocol 1 from a K562 cell with I_{Kr}-like currents before (*top* "control" traces) and after (*middle* "E4031" traces) exposure to 1 μM E4031. *Bottom* "E4031-sensitive" current traces of the cell were calculated by subtracting E4031 traces from control ones. Prepulse to +40 m*V* is not shown

Figure 2c shows the current traces at several voltages of a cell before and after exposure to the HERG blocker E4031, and the E4031-sensitive currents were calculated by subtracting the E4031-resistant currents from the control ones. Peak conductance showed inward rectification (Fig. 3a), while steady-state conductance did not (*data not shown*). At very negative potentials HERG1 channels revisit the open state briefly before closing; thus, the transient peak (P) tail current is conducted by open HERG1 channels plus other conductances, while the steady-state (SS) current is conducted only by other conductances (since HERG1 channels are closed). The ratio between P/SS currents allows estimation of the proportion of HERG1 currents with respect to the whole-cell currents for each cell. The P/SS ratio was measured in all cells where I_{Kr}-like currents were detected ($n = 81$, Fig. 3b). Nearly 75% of the P current was blocked by 1 μM E4031 since ≈ 25% of the whole-cell current remained after E4031 application, suggesting that three-fourths of the transient peak current was conducted by HERG1 channels. (P/SS ratio changed from ≈ 4 to ≈ 1 after drug exposure, $n = 27$, Fig. 3b.) The time necessary to reach P current (Fig. 3c) significantly decreased with hyperpolarization ($p < 0.01$), but no significant differences were found in the time necessary to reach P between control I_{Kr}-like currents and E4031-sensitive currents (Fig. 3c).

Cells with no detectable I_{Kr}-like currents showed no inward P current upon repolarization (at the same time interval), and their P/SS amplitude ratio was 1.05 ± 0.05 at −120 m*V* and 1.15 ± 0.05 at −60 m*V*. As expected, E4031 1 μM had no effect upon their currents ($n = 6$, *data not shown*).

Kinetics of the E4031-Sensitive Currents

Whole-cell currents were measured in the absence and presence of 1 μM E4031, and the E4031-sensitive currents were obtained by subtracting the E4031-resistant currents from the control ones. The time constants of recovery from inactivation and deactivation determined with protocol 1 are shown in Figure 3d, and the exact values are reported in Table 2 (for kinetic analysis only traces with tail length >1 s were used). The time constant of recovery from inactivation was voltage-dependent, increasing with depolarizing potentials ($p < 0.01$). Deactivation time constants seemed to steeply increase with depolarization as well, although significant differences were only found between −120 m*V* and the rest of the applied pulses.

Sensitivity to E4031

Half-maximal inhibitory concentration (IC_{50}) of the blocker was calculated by studying the effect of increasing concentrations of E4031 upon cells with I_{Kr}-like inward tail

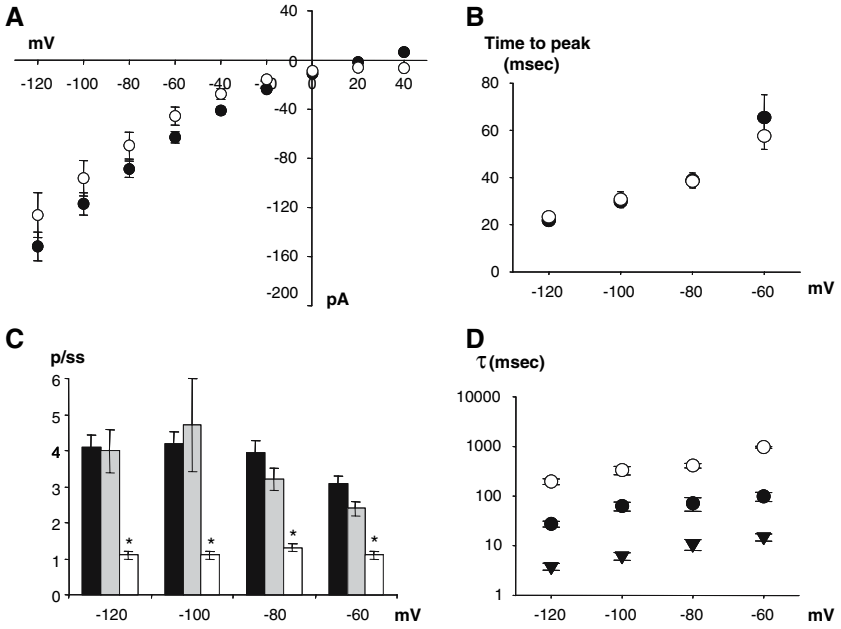

Fig. 3 Characterization and kinetics of HERG1 currents in K562 cells. **a** Mean tail peak conductance of control I_{Kr}-like currents (*black circles*, $n = 81$) and subtracted E4031-sensitive currents (*white circles*, $n = 27$) obtained with protocol 1. **b** Mean P/SS ratio at the voltages shown was calculated from control traces of all cells with I_{Kr}-like currents (*black bars*, $n = 81$) or from control and E4031 traces of cells with I_{Kr}-like currents exposed to E4031 (*gray* and *white bars*, respectively; $n = 27$) obtained with protocol 1. No significant differences were found between control P/SS values of the subset of cells having I_{Kr}-like currents tested with E4031 and the entire population of cells having I_{Kr}-like currents (*black vs. gray bars*, unpaired Student's *t*-test $p > 0.05$). E4031 P/SS values were significantly different with respect to control P/SS values (*gray vs. white bars*, $n = 27$, paired Student's *t*-test, $p < 0.05$). **c** Mean time necessary to reach peak tail current values at the voltages shown, calculated from control traces of all cells with I_{Kr}-like currents (*black circles*, $n = 81$) or from subtracted E4031-sensitive currents (*white circles*, $n = 27$), obtained with protocol 1. **d** Mean kinetic parameters of E4031-sensitive currents. *White circles* represent slow deactivation time constant (τs, $n = 4$–12), *black circles* represent fast deactivation time constant (τf, $n = 4$–12) and *filled triangles* represent recovery from inactivation time constant (τri, $n = 9$–12). Exact values are detailed in Table 2

Table 2 Mean ± SE time constants (τ) of deactivation and recovery from inactivation of the subtracted E4031-sensitive currents at various voltages (number of cells)

τ-deactivation	−120 m*V* (12)	−100 m*V* (11)	−80 m*V* (9)	−60 m*V* (4)
τ-fast (ms)	27.5 ± 3.7	59.2 ± 12.3	71.4 ± 22.1	81.6 ± 22.3
τ-slow (ms)	239.5 ± 35.9	316.0 ± 61.1	385.9 ± 45.4	407.2 ± 192.3

τ-recovery from inactivation	−120 m*V* (11)	−100 m*V* (12)	−80 m*V* (11)	−40 m*V* (9)
τ-ri (ms)	3.8 ± 0.6	6.2 ± 2.4	11.0 ± 2.4	15.1 ± 2.3

current. The fraction of I_{Kr}-like P current blocked by E4031 was calculated at −120 m*V* for each drug concentration and fitted with the Hill equation (see "Materials and Methods"). The E4031 maximum fractional block (FB_{max}) was 0.72 ± 0.02. That is, ≈72% of the whole-cell P current was blocked by E4031. The IC_{50} was 4.69 ± 0.63 nM, and the Hill coefficient was 1.00 ± 0.13 (Fig. 4a). Maximum block is achieved with 100 nM since *FB* values were not significantly different between drug concentrations ≥ 100 nM (ANOVA, $p > 0.05$). Figure 4b shows representative current traces of a cell exposed to no, 5 nM and 1 μM E4031.

Voltage Dependence of Activation of E4031-Sensitive Currents

To study the voltage dependence of activation of the HERG1 currents, protocol 2 was used (Fig. 4c), where the instant tail current was calculated and normalized to the maximum value ($I/I_{max} = p_o$). Three representative current traces obtained under this protocol are shown in Figure 4D. The fraction of open channels (p_o) was plotted for each preceding test pulse applied in Figure 4e. Voltage dependence of activation was calculated for whole-cell control currents and for E4031-sensitive currents by adjusting the

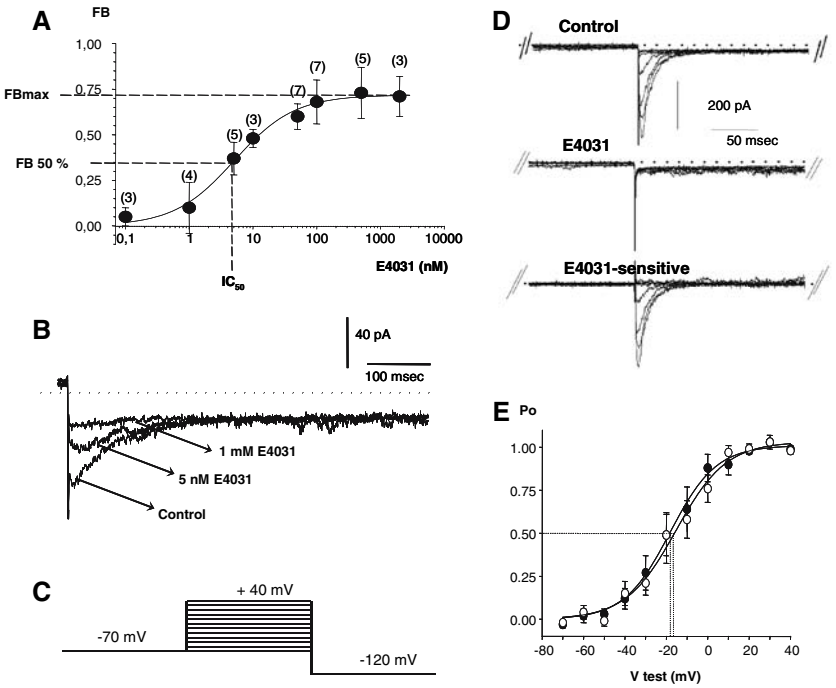

Fig. 4 Drug sensitivity and voltage-dependent activation of HERG1 currents in K562 cells. a E4031 dose-dependent blockade. In parentheses are shown the number of cells tested for each drug concentration. b Representative tail current traces of a cell exposed to 0 nM, 5 nM and 1 μM E4031 at -120 m*V*, obtained with protocol 1. For clarity, the time scale was amplified and prepulse to +40 m*V* is not shown. *Dotted line* represents 0 current levels. c Graphic representation of protocol 2, which consisted of a 2-s hyperpolarizing step to -70 m*V*, followed by a family of test pulses from -70 to +40 m*V* (400 ms) and a final hyperpolarizing step to -120 m*V* (300 ms). d Representative current traces obtained with protocol 2, from a cell with I_{Kr}-like currents before (*top* "control" traces) and after (*middle* "E4031" traces) exposure to 1 μM E4031. *Bottom* "E4031-sensitive" current traces of the cell were calculated by subtracting E4031 traces from control ones. Preconditioning pulse to -70 m*V* is not shown. For clarity, the time scale was amplified. *Dotted lines* represent 0 current levels. e Mean normalized instant currents ($I/I_{max} = p_o$), calculated at the hyperpolarizing -120 m*V* step, were plotted against the corresponding preceding test pulse and fitted with the Boltzmann equation. *White* and *black circles* correspond to control and E4031-sensitive values, respectively ($n = 7$, $p > 0.05$)

p_o curve with the Boltzmann equation (see "Materials and Methods"). As can be seen, there are no significant differences between control and E4031-sensitive currents: $V_{0.5}$ was -18.1 ± 4.7 m*V* and -16.6 ± 4.8 m*V* and z was 2.3 ± 0.7 and 2.2 ± 0.2 for control and E4031-sensitive currents, respectively ($n = 7$). Similarly, there were no differences in time constants of recovery from inactivation at -120 m*V* between control and E4031-sensitive currents (*data not shown*).

Effect of H_2O_2 on K562 Native HERG1 Currents

Hydrogen peroxide activates greatly homotetrameric HERG1a channels in heterologous expression systems (Berube, Caouette & Daleau, 2001; Wang et al., 2002; Han et al., 2004); however, its effect upon native I_{Kr} currents of different cell lines seems much more variable (Wang et al., 2002). Loss of intracellular K^+ because of the activation of HERG1 channels by reactive oxygen species is proposed to be an apoptotic signal (Wang et al., 2002; Han et al., 2004).

We studied the effect of H_2O_2 upon native HERG1 currents of K562 cells. Since there are no significant differences between voltage activation dependence, time to peak, P/SS ratio and inward conductance of control I_{Kr}-like currents and subtracted E4031-sensitive currents (Figs. 3, 4), we studied the H_2O_2 effect on native HERG1 channels of K562 cells by direct comparison of I_{Kr}-like currents before and after exposure to hydrogen peroxide.

Figure 5a shows a representative experiment before and after 10-min exposure to 400 μM H_2O_2, obtained with protocol 2. Voltage dependence of activation was calculated by fitting tail current with a Boltzmann equation as described previously (Fig. 5b). Voltage dependence of activation was not significantly different after H_2O_2 treatment ($V_{0.5} = -13.9 \pm 3.0$ and -15.1 ± 3.8 m*V*, $z = 2.5 \pm 0.4$ and 2.3 ± 0.2 for control and H_2O_2 currents, respectively; $n = 8$). Figure 5c shows representative tail current traces obtained with protocol 1 before and after exposure to 400 μM H_2O_2. No increase of whole currents was observed after H_2O_2 treatment; moreover, a small

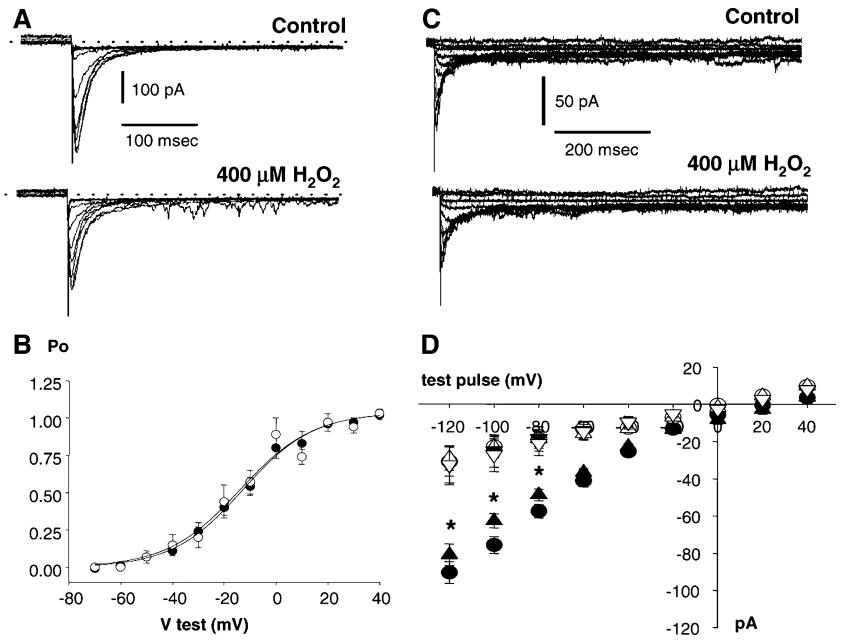

Fig. 5 Lack of H_2O_2 effect upon HERG1 currents in K562 cells. **a** Representative current traces obtained with protocol 2, from a cell with I_{Kr}-like currents before and after exposure to 400 μM H_2O_2 (*top* and *bottom traces*, respectively). Preconditioning pulse to −70 m*V* is not shown. For clarity, the time scale was amplified. *Dotted line* represents 0 current levels. **b** Mean normalized instant currents ($I/I_{max} = p_o$), calculated at the hyperpolarizing −120 m*V* step, were plotted against the corresponding preceding test pulse and fitted with the Boltzmann equation. *White* and *black circles* correspond to control and H_2O_2 values, respectively ($n = 8$, $p > 0.05$). **c** Representative current traces obtained with protocol 1 from a K562 cell with I_{Kr}-like currents before and after exposure to 400 μM H_2O_2 (*top* and *bottom traces*, respectively). Prepulse to +40 m*V* is not shown. **d** Mean peak and steady-state currents (*black* and *white symbols*, respectively) obtained with protocol 1 and plotted against the test pulse. *Circles, up triangles* and *down triangles* represent control ($n = 8$), 400 μM H_2O_2 ($n = 8$) and 400 μM H_2O_2 + 1 μM E4031 ($n = 4$) values, respectively. Statistically significant differences (*) were found between peak control and peak 400 μM H_2O_2 currents at voltages more negative than −60 m*V*

decrement in peak tail current (≈5%) was detected at voltages more negative than −80 m*V* (Fig. 5d), which could be due to an acceleration of the slow deactivation time constant (i.e., $\tau d = 248.5 \pm 58.8$ and 128.3 ± 38.3 for control and H_2O_2, respectively, at −120 m*V*; $n = 6$, $p < 0.05$). Subsequent exposure to 1 μM E4031 inhibited peak I_{Kr}-like currents (Fig. 5d). No differences were found in steady-state currents, suggesting the lack of H_2O_2 effect on other conductances (Fig. 5d). Nevertheless, in another set of experiments, E4031 1 μM was applied prior to hydrogen peroxide to discard a possible H_2O_2 effect upon other non-HERG1 currents. The E4031-resistant currents were not affected by 400 μM H_2O_2 ($n = 6$, $p > 0.05$; *data not shown*). Inactivation was studied with a protocol consisting of an activating pulse to 40 m*V* (400 ms) followed by a 15–20 ms step to −120 m*V* to allow recovery from inactivation and a family of pulses from 10 to 40 m*V* (in 10-m*V* steps), at which the time constant of inactivation (τi) was calculated by fitting the current decay to a single exponential function. Inactivation was accelerated after H_2O_2 treatment at all voltages ($\tau i = 9.97 \pm 0.67$ and 6.00 ± 0.94 ms at 10 m*V* for control and H_2O_2, respectively; $n = 3$, $p < 0.05$). This change could also account for the observed current decrease.

Immunoprecipitation of HERG Isoforms in K562 Cells

The results obtained with PCR, Western blots and patch-clamp experiments suggest that K562 cells express HERG1a and HERG1b proteins on their plasma membrane. In order to explore the possibility that these two isoforms coassemble, bidirectional immunoprecipitation was carried out in K562 protein extracts; and the entire blot membrane is shown in Figure 6. In these cells, the mature glycosylated form of HERG1a protein (∼155 kDa) was immunoprecipitated with HERG1b-specific antibody (Fig. 6a). On the other hand, Figure 6b shows the HERG1b mature form (∼95 kDa) immunoprecipitated with the HERG1a antibody. These results suggest that both HERG isoforms are physically associated in K562 cells.

Discussion

In the present work we show that K562 cells express two isoforms of the herg1 gene (1a and 1b), which successfully translate into proteins as demonstrated with RT-PCR and Western blot experiments. Different states of glycosylation were observed for the HERG1a and HERG1b proteins,

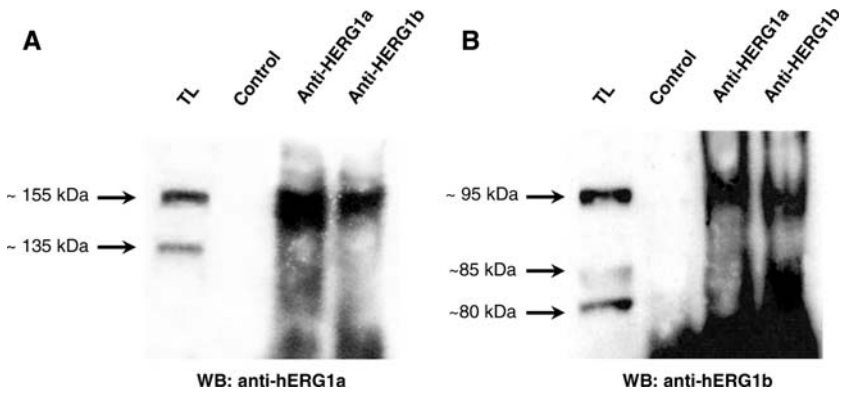

Fig. 6 Physical association between HERG1a and HERG1b isoforms in K562 cells. Each line indicates total K562 protein extracts immunoprecipitated with amino-terminal-specific antibodies and immunoblotted (*WB*) using HERG1a or HERG1b antibodies. *Lane TL*, total protein lysates; for a negative control, total rabbit serum was used. The HERG1b antibody immunoprecipitated a ~155-kDa 1a band (**a**) and the HERG1a antibody immunoprecipitated a ~95-kDa 1b band (**b**)

consistent in size with previously published results for this channel (Zhou et al., 1998; Petrecca et al., 1999; Crociani et al., 2003; Jones et al., 2004).

Channel function was studied with the patch-clamp technique in the whole-cell configuration. To isolate and identify the native HERG1 currents of K562 cells, we applied two commonly used protocols in combination with E4031, which selectively blocks HERG1 channels. K562 HERG1 currents were blocked by E4031 with an IC_{50} of 4.69 ± 0.63 nM; the Hill coefficient was 1, indicating that a single E4031 molecule interacts with one channel molecule. The blocking potency of E4031 varies when comparing native and heterologous expression systems and even among different expression systems; this variability seems to be influenced by the voltage pulse at which drug equilibration is allowed, as well as by the ionic conditions used or the association with auxiliary β-subunits (Abbott et al., 1999; Spector et al., 1996b; Wang et al., 1997b). In mouse, E4031 blocked ERG1b channels with higher affinity than ERG1a channels, its IC_{50} value being ≈300 *vs.* ≈490 μM (London et al., 1997). The E4031 IC_{50} value for HERG1a channels heterologously expressed in mammalian cells was reported to be 7.7–8.8 nM (Zhou et al., 1998; Abbott et al., 1998), although much higher values were reported for native I_{Kr} currents (Sanguinetti & Jurkiewicz, 1990). The HERG1a N terminus is known to modulate channel kinetics by interacting either directly or indirectly with other channel regions (Wang et al., 1998; Sanguinetti & Xu, 1999; Zhang et al., 2005; Aydar & Palmer, 2001) or with other proteins (Kagan et al., 2002) and to be involved in channel assembly (Li, Xu & Li, 1997; Paulussen et al., 2002). Homotetrameric WT ERG1a channels as well as N-terminally deleted ERG1a channels have been abundantly studied in different expression systems. Removal of the N terminus produces an acceleration in time deactivation constants (Spector et al., 1996a; Schönherr & Heinemann, 1996; Morais-Cabral et al., 1998; Wang et al., 1998), which can be restored by addition of a complete or partial N-terminal peptide (Morais-Cabral et al., 1998; Wang, Myers & Robertson, 2000). N-terminal deletion effects can be mimicked by mutations in the S4-S5 intracellular linker (Wang et al., 1998; Sanguinetti & Xu, 1999). However, native ERG1b subunits do not efficiently produce surface membrane homotetramers (London et al., 1997; Robertson, Jones & Wang, 2005), which is why this type of channel is less characterized. Nevertheless, they are known to display differential kinetics compared to ERG1a homotetramers or ERG1a/1b heterotetramers (Lees-Miller et al., 1997; London et al., 1997; Robertson et al., 2005; Kirchberger et al., 2006). We characterized several kinetic parameters of the HERG1 currents of K562 cells. When compared with published data obtained under similar ionic and temperature conditions, we observed that native HERG1 currents had a $V_{0.5}$ of activation similar to heterotetrameric I_{Kr} current of ventricular myocytes (Li et al., 1997). Deactivation time constants were very similar to native I_{Kr} of guinea pig myocytes (Sanguinetti & Jurkiewicz, 1990), being slightly slower than homotetrameric N-truncated ERG1a or ERG1b channels (Spector et al., 1996a; Lees-Miller et al., 1997; Wang et al., 1998) but much faster than WT HERG1a homotetramers (Sanguinetti et al., 1995; Spector et al., 1996a; Wang et al., 1998). Thus, our patch-clamp data support that in K562 cells both subunits coassemble into heteromultimeric HERG1a/b channels, with some properties being dominated by one subunit and other properties having intermediate values. To confirm these results, we performed immunoprecipitation experiments in which we observed a physical association between the mature forms of HERG1a and HERG1b in this cell line.

Within the N terminus of ERG1a there is a highly conserved PAS (*Per, Arnt, Sim)* domain, which is involved in protein-protein interactions in other eukaryotic proteins (Morais Cabral et al., 1998). Also, PAS domains of prokaryote proteins are known to have sensory properties, such as sensing the cellular oxidative status of the cell (Morais-Cabral et al., 1998). Reactive oxygen species are reported to modulate HERG1 currents, although the percentage of change and the kinetic parameter affected varied markedly between reports, perhaps depending on the expression system, the oxidizing agent or the concentration used (Taglialatela et al., 1997; Berube et al., 2001; Wang et al., 2002; Pannaccione et al., 2002; Han et al., 2004). Expressed HERG1a currents are increased by H_2O_2 (Berube et al., 2001; Wang et al., 2002; Han et al., 2004). There is no report of an H_2O_2 effect on expressed ERG1b or ERG1a/b channels, but variable current increase is reported in cell lines known to express both isoforms of the gene (Wang et al., 2002). We found that K562 I_{Kr}-like whole-cell currents were not activated by H_2O_2. We do not know for sure the reason for this discrepancy. It could be that cells expressing both HERG1 isoforms respond differently to H_2O_2 depending on the proportion of homo- and heterotetrameric channels they possess. Also, the existence of genetic polymorphism between the channels of each cell line (Anson et al., 2004) and interactions with other proteins or auxiliary β-subunits differentially expressed in each cell type (Abbott et al., 1999) may affect reactive oxygen species sensitivity.

It has been proposed that HERG1 currents participate in the regulation of tumor cell invasiveness, control of tumor cell neoangiogenesis and apoptotic cascade signaling by modulating the intracellular concentration of K^+ (Wang et al., 2002; Han et al., 2004; Arcangeli, 2005). HERG1 channels are implicated in cell proliferation based on the effect of HERG blockers. E4031 impaired proliferation of neuroblastoma and neoplastic hematopoietic cells (Smith et al., 2002; Crociani et al., 2003), although the concentration of E4031 used was much higher that the IC_{50} required to block HERG currents. Similar results were obtained with WAY 123,398, another HERG current blocker (Pillozzi et al., 2002). HERG1 channels are also implicated in the regulation of cell proliferation, especially in leukemias by clamping the membrane voltage (V_r) to a depolarized potential characteristic of proliferating immature cells (*for review, see* Arcangeli, 2005). Since HERG1 homo- and heterotetramers display differential kinetics, fine-tuned modulation of V_r, and thus of proliferation or apoptosis signaling, might be dependent on the expressed ratio of these isoforms. Perhaps K562 cells express a higher proportion of HERG1b than HERG1a isoform, favoring the formation of heterotetrameric channels insensitive to reactive oxygen species, thus modulating proliferation without increasing the apoptosis sensitivity of the cells to reactive oxygen species.

Acknowledgment We thank Dr. C. January (Department of Medicine, University of Wisconsin, Madison, WI) for the gift of herg1a stably transfected HEK293 cells and Dr. Gail A. Robertson (University of Wisconsin, Madison, WI) for the gift of antibodies for the HERG1a and HERG1b isoforms. We extend out thanks to Dr. Felisa C. Molinas and Dr. Mónica Costas (Instituto de Investigaciones Médicas Alfredo Lanari) for lab facilities and Dr. R. Kass (Columbia University, New York, NY) for the gift of drugs and reactives. M. S. C., S. M. d.M. and Y. A. A. are fellows of the National Council of Research of Argentina (CONICET). C. I. and B. A. K. are established investigators of CONICET.

References

Abbott GW, Sesti F, Splawski I, Buck ME, Lehmann MH, Timothy KW, Keating MT, Goldstein SAN (1999) MiRP1 forms I_{Kr} potassium channels with HERG and is associated with cardiac arrhythmia. Cell 97:175–187

Anson BD, Ackerman MJ, Tester DJ, Will ML, Delisle BP, Anderson CL, January CT (2004) Molecular and functional characterization of common polymorphisms in HERG (KCNH2) potassium channels. Am J Physiol 286:H2434–H2441

Arcangeli A (2005) Expression and role of hERG channels in cancer cells. Novartis Found Symp 266:225–234

Assef YA, Kotsias BA (2002) An outwardly rectifying anion channel in human leukaemic K562 cells. Pfluegers Arch 444:816–820

Assef Y, Damiano A, Zotta E, Ibarra C, Kotsias BA (2003) CFTR in K562 human leukemic cells. Am J Physiol 285:C480–C488

Assef YA, Cavarra MS, Damiano AE, Ibarra C, Kotsias BA (2005) Ionic currents in multidrug resistant K562 human leukemic cells. Leuk Res 29:1039–1047

Aydar E, Palmer C (2001) Functional characterization of the C-terminus of the human ether-a-go-go-related gene K^+ channel (HERG). J Physiol 534:1–14

Bauer CK, Wulfsen I, Schäfer R, Glassmeier G, Wimmers S, Flitsch J, Lüdecke DK, Schwarz JR (2003) HERG K^+ currents in human prolactin-secreting adenoma cells. Pfluegers Arch 445:589–600

Berube J, Caouette D, Daleau P (2001) Hydrogen peroxide modifies the kinetics of HERG channel expressed in a mammalian cell line. J Pharmacol Exp Ther 297:96–102

Crociani O, Cherubini A, Piccini E, Polvani S, Costa S, Fontana L, Hofmann G, Rosati B, Wanke E, Olivotto M, Arcangeli A (2000) Erg gene(s) expression during development of the nervous and muscular system of quail embryos. Mech Dev 95:239–243

Crociani O, Guasti L, Balzi M, Becchetti A, Wanke E, Olivotto M, Wymore RS, Arcangeli A (2003) Cell cycle-dependent expression of HERG1 and HERG1b isoforms in tumor cells. J Biol Chem 278:2947–2955

Curran ME, Splawski I, Tomothy KW, Vincent GM, Green ED, Keating MT (1995) A molecular basis for cardiac arrhythmia: HERG mutations cause long QT syndrome. Cell 80:795–803

Hamada H, Tsuruo T (1988) Purification of the 170–180-kilodalton membrane glycoprotein associated with multidrug resistance. J Biol Chem 263:1454–1458

Han H, Wang J, Zhang Y, Long H, Wang H, Xu D, Wang Z (2004) HERG K^+ channel conductance promotes H_2O_2 induced apoptosis in HEK293 cells: cellular mechanisms. Cell Physiol Biochem 14:121–134

Hoffman R, Murnane MJ, Benz EJ, Prohaska R, Floyd V, Dainiak N, Forget BG, Furthmayr H (1979) Induction of erythropoietic

colonies in a human chronic myelogenous leukemia cell line. Blood 54:1182–1187

Itoh T, Tanaka T, Nagai R, Kamiya T, Sawayama T, Nakayama T, Tomoike H, Sakurada H, Yazaki Y, Nakamura Y (1998) Genomic organization and mutational analysis of HERG a gene responsible for familial long QT syndrome. Hum Genet 102:435–439

Jones EMC, Roti Roti EC, Wang J, Delfosse SA, Robertson GA (2004) Cardiac I_{Kr} channels minimally comprise hERG 1a and 1b. J Biol Chem 279:44690–44694

Kagan A, Melman YF, Krumerman A, McDonald TV (2002) 14-3-3 amplifies and prolongs adrenergic stimulation of HERG K^+ channel activity. EMBO J 21:1889–1898

Kirchberger NM, Wulfsen I, Schwarz JR, Bauer CK (2006) Effects of TRH on heteromeric rat erg1a/b K^+ channels are dominated by the rerg1b subunit. J Physiol 571:27–42

Klein E, Ben-Bassat H, Neumann H, Ralph P, Zeuthen J, Polliack A, Vanky F (1976) Properties of the K562 cell line, derived from a patient with chronic myeloid leukemia. Int J Cancer 18:421–431

Kupershmidt S, Snyders DJ, Raes A, Roden DM (1998) A K^+ channel splice variant common in human heart lacks a C-terminal domain required for expression of rapidly activating delayed rectifier current. J Biol Chem 273:27231–27235

Lees-Miller JP, Kondo C, Wang L, Duff HJ (1997) Electrophysiological characterization of an alternatively processed ERG K^+ channel in mouse and human hearts. Circ Res 81:719–726

Li GR, Feng J, Yue L, Carrier M, Nattel S (1996) Evidence for two components of delayed rectifier K^+ current in human ventricular myocytes. Circ Res 78:689–696

Li X, Xu J, Li M (1997) The human D1261 mutation of the HERG potassium channel results in a truncated protein that contains a subunit interaction domain and decreases the channel expression. J Biol Chem 272:705–708

London B, Trudeau MC, Newton KP, Beyer AK, Copeland NG, Gilbert DJ, Jenkins NA, Satler CA, Robertson GA (1997) Two isoforms of the mouse ether-a-go-go–related gene coassemble to form channels with properties similar to the rapidly activating component of the cardiac delayed rectifier K^+ current. Circ Res 81:870–878

Lozzio CB, Lozzio BB (1975) Human chronic myelogenous cell line with positive Philadelphia chromosome. Blood 45:321–334

Morais Cabral JH, Lee A, Cohen SL, Chait BT, Li M, Mackinnon R (1998) Crystal structure and functional analysis of the HERG potassium channel N terminus: a eukaryotic PAS domain. Cell 95:649–655

Pannaccione A, Castaldo P, Ficker E, Annunziato L, Tagliatela M (2002) Histidines 578 and 587 in the S5-S6 linker of the human ether-a-gogo related gene-1 K^+ channels confer sensitivity to reactive oxygen species. J Biol Chem 277:8912–8919

Paulussen A, Raes A, Matthijs G, Snyders DJ, Cohen N, Aerssens J (2002) A novel mutation (T65P) in the PAS domain of the human potassium channel HERG results in the long QT syndrome by trafficking deficiency. J Biol Chem 277:48610–48616

Petrecca K, Atanasiu R, Akhavan A, Shrier A (1999) *N*-Linked glycosylation sites determine HERG channel surface membrane expression. J Physiol 515:41–48

Pillozzi S, Brizzi MF, Balzi M, Crociani O, Cherubini A, Guasti L, Bartolozzi B, Becchetti A, Wanke E, Bernabei PA, Olivotto M, Pegoraro L, Arcangeli A (2002) HERG potassium channels are constitutively expressed in primary human acute myeloid leukemias and regulate cell proliferation of normal and leukemic hemopoietic progenitors. Leukemia 16:1791–1798

Robertson GA, Jones EMC, Wang J (2005) Gating and assembly of heteromeric hERG1a/1b channels underlying I_{Kr} in the heart. Novartis Found Symp 266:4–18

Rutherford TR, Clegg JB, Weatherall DJ (1979) K562 human leukaemic cells synthesise embryonic haemoglobin in response to haemin. Nature 280:164–165

Sanguinetti MC, Jurkiewicz NK (1990) Two components of cardiac delayed rectifier K^+ current. Differential sensitivity to block by class III antiarrhythmic agents. J Gen Physiol 96:195–215

Sanguinetti MC, Chang J, Curran ME, Keating MT (1995) A mechanistic link between an inherited and an acquired cardiac arrythmia: HERG encodes the I_{Kr} potassium channel. Cell 81:299–307

Sanguinetti MC, Xu QP (1999) Mutations of the S4-S5 linker alter activation properties of HERG potassium channels expressed in *Xenopus* oocytes. J Physiol 514:667–675

Schönherr R, Heinemann SH (1996) Molecular determinants for activation and inactivation of HERG, a human inward rectifier potassium channel. J Physiol 493:635–642

Schwarz JR, Bauer CK (2004) Functions of erg K^+ channels in excitable cells. J Cell Mol Med 8:22–30

Shoeb F, Malykhina AP, Akbarali HI (2003) Cloning and functional characterization of the smooth muscle ether-a-go-go-related gene K^+ channel. Potential role of conserved amino acid substitution in the S4 region. J Biol Chem 278:2503–2514

Smith GAM, Tsui HW, Newell EW, Jiang X, Zhu XP, Tsui FWL, Schlichter LC (2002) Functional upregulation of HERG K^+ channels in neoplastic hematopoietic cells. J Biol Chem 277:18528–18534

Spector PS, Curran ME, Zou A, Keating MT, Sanguinetti MC (1996a) Fast inactivation causes rectification of the I_{Kr} channel. J Gen Physiol 107:611–619

Spector PS, Curran EC, Keating MT, Sanguinetti MC (1996b) Class III antiarrhythmic drugs block HERG, a human cardiac delayed rectifier K^+ channel. Open channel block by methanesulfonanilides. Circ Res 78:499–503

Taglialatela M, Castaldo P, Iossa S, Pannaccione A, Fresi A, Ficker E, Annunziato L (1997) Regulation of the human ether-a-gogo related gene (HERG) K^+ channels by reactive oxygen species. Proc Natl Acad Sci USA 94:11698–11703

Tsiftsoglou AS, Wong W, Tsamadou AI, Robinson SH (1991) Cooperative effects of hemin and anthracyclines in promoting terminal erythroid maturation in K562 human erythroleukemia cells. Exp Hematol 19:928–933

Wang L, Feng ZP, Kondo CS, Sheldon RS, Duff HJ (1996) Developmental changes in the delayed rectifier K^+ channels in mouse heart. Circ Res 79:79–85

Wang S, Liu S, Morales MJ, Strauss H, Rasmusson RL (1997a) A quantitative analysis of the activation and inactivation kinetics of HERG expressed in *Xenopus* oocytes. J Physiol 502:45–60

Wang S, Morales MJ, Liu S, Strauss HC, Rasmusson RL (1997b) Modulation of HERG affinity for E-4031 by $[K^+]_o$ and C-type inactivation. FEBS Lett 417:43–47

Wang J, Trudeau MC, Zappia AM, Robertson GA (1998) Regulation of deactivation by an amino terminal domain in human ether-a-go-go-related gene potassium channels. J Gen Physiol 112:637–647

Wang J, Myers CD, Robertson GA (2000) Dynamic control of deactivation gating by a soluble amino-terminal domain in HERG K^+ channels. J Gen Physiol 115:749–758

Wang H, Zhang Y, Cao L, Han H, Wang J, Yang B, Nattel S, Wang Z (2002) HERG K^+ channel, a regulator of tumor cell apoptosis and proliferation. Cancer Res 62:4843–4848

Wang Z (2004) Roles of K^+ channels in regulating tumour cell proliferation and apoptosis. Pfluegers Arch 448:274–286

Warmke JW, Ganetzky B (1994) A family of potassium channel genes related to eag in *Drosophila* and mammals. Proc Natl Acad Sci USA 91:3438–3442

Zhang M, Liu J, Jiang M, Wu DM, Sonawane K, Guy HR, Tseng GN (2005) Interactions between charged residues in the

transmembrane segments of the voltage-sensing domain in the hERG channel. J Membr Biol 207:169–181

Zhou Z, Gong Q, Ye B, Fan Z, Makielski JC, Robertson GA, January CT (1998) Properties of HERG channels expressed in HEK cells studied at physiological temperature. Biophys J 74:230–241

Zou A, Curran ME, Keating MT, Sanguinetti MC (1997) Single HERG delayed rectifier K^+ channels expressed in *Xenopus* oocytes. Am J Physiol 272:Hl309–Hl314